EBGM VS SUBSPACE PROJECTION FOR FACE RECOGNITION

Andreas Stergiou, Aristodemos Pnevmatikakis, Lazaros Polymenakos
Athens Information Technology
19.5 Km Markopoulou Avenue, P.O. Box 68, Peania, Athens, Greece

Keywords: Human-Machine Interfaces, Computer Vision, Face Recognition.

Abstract: Autonomic human-machine interfaces need to determine the user of the machine in a non-obtrusive way. The identification of the user can be done in many ways, using RF ID tags, the audio stream or the video stream to name a few. In this paper we focus on the identification of faces from the video stream. In particular, we compare two different approaches, linear subspace projection from the appearance-based methods, and Elastic Bunch Graph Matching from the feature-based. Since the intended application is restricted to indoor multi-camera setups with collaborative users, the deployment scenarios of the recognizer are easily identified. The comparison of the methods is done using a common test-bed for both methods. The test-bed is exhaustive for the deployment scenarios we need to consider, leading to the identification of deployment scenarios for which each method is preferable.

1 INTRODUCTION

The problem of face recognition on still images has gained much attention over the past years. One of the main driving factors for this trend is the ever growing number of applications that an efficient and resilient recognition technique can address, such as security systems based on biometric data and user-friendly human-machine interfaces. Example applications of the latter are smart rooms (Waibel et al., 2004), where the presence of humans and their identity is detected from video feeds. Although many algorithms for face recognition have been proposed (Zhao et al., 2000; Brunelli and Poggio, 1993; Turk and Pentland, 1991; Belhumeur et al., 1997; Gunning and Murphy, 1992; Wiskott et al., 1999), their performance depends on how unconstrained the environment is (variations in pose, illumination, and expression (Belhumeur et al., 1997; Georghiades et al., 2001; Martinez and Kak, 2001), as well as partial face occlusion (Pentland et al., 1994)) and on geometric face normalization. Hence, finding a resilient, all-purpose face recognition method has proven a tough challenge.

An overview of algorithms for both still- and video-based face recognition is presented in (Zhao et al., 2000). A broad categorization of the algorithms is based on the way they treat an image; as a whole (appearance-based), or in terms of specific, easily identifiable points on the face (feature-based) (Brunelli and Poggio, 1993). The most well-known and studied appearance-based methods are the linear subspace projection methods: The Eigenface method (Turk and Pentland, 1991) employs Principal Component Analysis (PCA) (Duda et al., 2000), and the Fisherface method (Belhumeur et al., 1997) couples that with Linear Discriminant Analysis (LDA) (Duda et al., 2000) to improve performance. Many variants of these methods exist (Pentland et al., 1994). Feature-based approaches include neural networks (Gunning and Murphy, 1992) and Elastic Bunch Graph matching (EBGM) (Wiskott et al., 1999).

The aim of this paper is to compare EBGM from the feature-based approaches with the linear subspace projection methods from the appearance-based approaches. The comparison addresses both performance and suitability for real-time application. Since the performance of PCA+LDA under different distance metrics and number of training images has been studied (Pnevmatikakis and Polymenakos, 2004; Beveridge and She, 2001), the same is needed for EBGM. Different identification metrics and number of training images per subject are utilized to obtain identification rates, as well as the ability of EBGM to automatically locate the facial features of interest on the images. The latter is very important since the overall system success depends on accurate feature localization. This set of experiments establishes a baseline performance for EBGM. Further experiments are conducted to study the effect on the baseline of varying image sizes and offsets in the eye positions caused by imperfect eye detection. The algorithm is implemented in SuSe Linux 9.1 using the RAVL C++ libraries (Christmas and Galambos, 2005) from the University of Surrey.

Stergiou A., Pnevmatikakis A. and Polymenakos L. (2006).
EBGM VS SUBSPACE PROJECTION FOR FACE RECOGNITION.
In *Proceedings of the First International Conference on Computer Vision Theory and Applications*, pages 131-137
DOI: 10.5220/0001359401310137

The paper is organized as follows: Section 2 gives an overview of the EBGM algorithm. Section 3 discusses the image preprocessing and feature estimation stages. Section 4 describes the face database used; the baseline EBGM performance is identified and compared to subspace projection methods. Section 5 extends the comparison to different preprocessing schemes and impairments like face size and inaccurate eye position. Conclusions are drawn in Section 6, along with guidelines for extensions of EBGM.

2 EBGM OVERVIEW

EBGM assumes that the positions of certain facial features (termed fiducial points in (Wiskott et al., 1999)) are known for each image in the database. Information on each face is collected by convolving the image regions around these fiducial points with 40 complex 2D Gabor kernels. Gabor wavelets are formed by multiplying a sinusoidal with a Gaussian function. The Gaussian has a dampening effect, hence only pixel values near the given fiducial point contribute to the convolution. The resulting 80 coefficients constitute the Gabor jet for each fiducial point. The Gabor jets for all fiducial points are grouped in a graph, the Face Graph, where each jet is a node and the distances between fiducial points are the weights on the corresponding vertices. The information in the Face Graph is all that is needed for recognition; the image itself is discarded.

All Face Graphs from the training images are combined in a stack-like structure called the Face Bunch Graph (FBG). Each node of the FBG contains a list of Gabor jets for the corresponding fiducial point from all training images, and the vertices are now weighted with the average distances across the training set. The exact positions of the fiducial points on the training images are known.

The positions of the fiducial points in the testing images are unknown; EBGM estimates them based on the FBG. Then a Face Graph can be constructed for each testing image based on the estimated fiducial point positions. The Face Graph of each testing image is compared with the FBG to determine the training image it is most similar with, according to some jet-based metric.

3 PREPROCESSING, FACE GRAPHS AND RECOGNITION

Although in principle EBGM can handle some scale, shift and rotation between the faces, to be fair in the comparison with the PCA+LDA method that needs normalization (Pnevmatikakis and Polymenakos, 2004), the images are normalized according to the eye positions. Hence effectively the eye positions are known also for the testing images.

The normalization involves scaling, rotation and shifting. The goal is to bring the face at the center of the image, rotate and resize it appropriately so that the eyes are aligned at preselected positions and at a predefined distance. The normalization parameters (eye coordinates and distance) are selected so that convolution with even the largest kernel does not extend outside the image border. Then, the remaining background is discarded by cropping a rectangular area around the face. To avoid abrupt intensity variations at the cropped image border which disrupt the convolution results, the intensity around the face is smoothed as proposed in (Bolme, 2003).

The localization of the fiducial points is done in two steps: initial estimation and refinement. The initial estimation is based on the positions of the previously localized face features. Starting with the positions of the eyes (which are accurately positioned after normalization), an estimate for the position of the n-th point is obtained by the weighted average

$$\vec{p_n} = \frac{\sum_{i=1}^{n-1} w_{in}(\vec{p_i} + \vec{v_{in}})}{\sum_{i=1}^{n-1} w_{in}} \quad (1)$$

where $\vec{p_i}$ are the positions of the *n-1* previously estimated points, $\vec{v_{in}}$ are the average distance vectors between points *i* and *n* from the FBG and $w_{in} = e^{-\|\vec{v_{in}}\|}$ are weighting factors that give more weight to neighboring features. The sequence of localization in (Bolme, 2003) is from the eyes radially outwards to the edge of the face, but our experiments indicate that this does not improve estimation accuracy; any order can be used.

The refinement step improves the initial estimate accuracy by using Gabor jet similarity metrics (Bolme, 2003). The Gabor jet from the initial estimate is compared to all jets in the FBG for that fiducial point. The jet from the FBG with the highest similarity is the local expert. The best metric to estimate the local expert is the Phase Similarity. The local expert is used for the refinement of the position of the fiducial point in the testing image, based on the maximization of the Displacement Similarity metric as a function of the displacement between the current jet of the testing image and its local expert. Four different maximization methods are presented in (Wiskott et al., 1999; Bolme, 2003).

After the fiducial points for a testing image have been estimated, Gabor jets are extracted from all those positions to construct the testing Face Graph. The latter is compared against all training Face Graphs in the FBG to obtain the identity of the person. A number of metrics are proposed in (Wiskott et al., 1999; Bolme,

2003) for this comparison.

The simplest metric is to ignore all information in the Face Graph nodes (the jets) and rely only on that of the vertices of the Face Graph (the positions of the fiducial points). A scan across the FBG produces the member for which the average (across all features) Euclidean distance from the testing Face Graph is minimized. This is the Geometry Similarity (GeoS). Although extremely fast, this metric gives the worst results by far. This is due to the normalization step which enforces a uniform distribution of the facial features across all images, making a successful identification very difficult even when a very large number of training images per class are available.

The main drawback of GeoS is that it does not utilize the information about the surrounding areas of the fiducial points stored in the Gabor jets. The simplest methods that make use of this information are Magnitude Similarity (MS) and Phase Similarity (PS), discussed in (Wiskott et al., 1999; Bolme, 2003).

A family of more sophisticated metrics is based on the Displacement Estimation (DE) methods already discussed. Again we try to find a displacement vector for the testing Gabor jet that would maximize its similarity to the corresponding training jet under the Displacement Similarity metric. The difference now is that the training jets in the maximization of the metric for all nodes in the testing Face Graph are nodes of the same member of the FBG and not the local experts of the testing jets.

4 BASELINE PERFORMANCE FOR EBGM

For our experiments with EBGM the HumanScan face database (Jesorsky et al., 2001) is used. This data set consists of 1,521 grayscale images, corresponding to 23 different individuals. In some images part of the face is missing; these images are discarded leading to a total of 1,373 images belonging to 21 distinct classes. For each image, the coordinates of 20 hand-annotated fiducial points are provided. These coordinates are used both in the image preprocessing phase and in the FBG creation. There is a lot of within-class diversity, as the database contains images with variations in illumination, pose (faces are mostly frontal, but with tilts), expression and occlusions (glasses or hands). Unfortunately these variations are not performed systematically; hence any given impairment is not guaranteed to exist across all subjects nor with the same intensity. This necessitates reporting of the performance as an average across many runs with different selection of training images.

The goal of the experiments carried out in this section is to establish a baseline performance for EBGM under normal training/testing conditions. By normal (but not ideal) conditions we define images that are approximately frontal and with mostly neutral expressions. The only occlusions allowed are normal glasses (not dark sunglasses) and blinking eyes. Lighting conditions may vary, but not to the extreme. Hence the HumanScan database is suitable for the baseline performance determination. Note that, unless otherwise stated, the eyes have been manually located, allowing for the testing of the face recognition algorithms in the semi-automatic manner, ignoring the task of automatic face detection (Yang et al., 2002).

4.1 Refinement of Fiducial Point Position

Experiments have been carried out to determine the optimum DE method in terms of accuracy and speed. Accuracy is measured based on the average RMS estimation error across all features and the whole test image set. Speed is measured as the average time for fiducial point position estimation per image. The DEPS (DE Prediction Step) method has no parameters; for the other three the chosen parameter values are as follows: The maximum number of iterations for DEPI (DE Predictive Iteration) is 3, 6 and 10, the grid size for DEGS (DE Grid Search) is 8, 12 and 16 pixels, and the maximum number of search steps for DELS (DELocal Search) is 10, 25 and 50. The experiments were run on a P4/2.66GHz with 512 MB RAM under SuSe Linux 9.1. (Bolme, 2003) summarizes the key characteristics of each of the four DE methods.

The results in terms of Average Processing Time (APT) are presented in Figure 1 as a function of the number of training images per class. For the three parametric methods, the version that gave the best results in each case is shown (i.e., DEPI_3, DEGS_8 and DELS_10). It is clear that DEPI_3 is by far the slowest DE method, whereas the other three have very small speed discrepancies. The results are justified as the bulk of the processing time for feature estimation is taken up by the convolutions with the Gabor kernels. Hence DEPS, DEGS_8 and DELS_10 have comparable run times while DEPI_3, which involves more than one convolution steps, is slower.

The average RMS error over all facial features is shown in Figure 2. For all three parametric methods, the parameter value that resulted in faster processing time also gives the most accurate estimation. For DEPI this is due to the fact that more than three iterations are rarely needed. A similar argument holds for DELS, while for DEGS the answer lies in the image normalization. Since the preprocessing stage leads to a more or less standard face size and orientation, it is expected that maximization is achieved close to the initial estimate; therefore increasing the search area

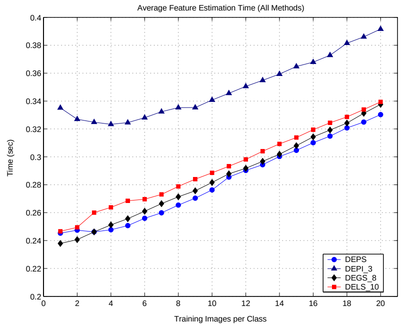

Figure 1: APT for the four DE methods.

has little impact on performance and may even lead to higher errors if a feature is falsely estimated to lie farther away from the staring point. Based on its superior performance in terms of RMS error and its fast run times, DELS_10 is chosen as the DE method.

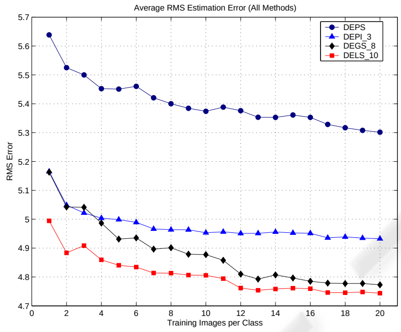

Figure 2: Average RMS error across all facial features for the four DE methods.

4.2 Testing Face Graph Similarity with FBG

The identification performance of the EBGM algorithm is evaluated based on a variety of Gabor Jet similarity metrics, discussed in (Bolme, 2003). For the local expert identification, the jet phase utilized in the PS metric yields much better results than the magnitude utilized in the MS metric. This is not the case for determining the FBG member that is most similar to a testing Face Graph (Wiskott et al., 1999). This fact is verified in Figure 3, where the performance of both MS and PS for a single run with between 1 and 24 training images per class is shown. Although a single run can be misleading, the performance gap between the two metrics is enough to disregard PS from the rigorous experimentation that follows.

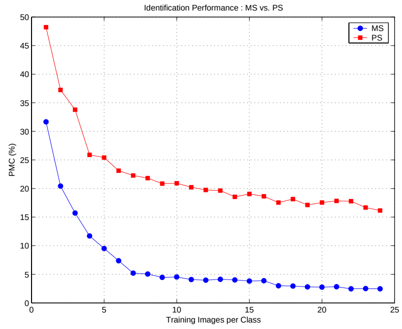

Figure 3: Comparison of identification performance in terms of PMC for the MS and PS metrics.

The use of the DS (Displacement Similarity) metric for determining the FBG member that is most similar to a testing Face Graph is more promising. From the four variants, DEPI is not studied because it is excessively slow. The recognition performance in terms of the Probability of Misclassification (PMC), averaged over 25 runs with a single training image per class, together with the identification times, are listed in Table 1 for GeoS, MS, PS, DEPS, DEGS_16 and DELS_25.

Table 1: Comparison of six different similarity metrics across 25 runs with 1 training image per class. Average PMC and recognition times are reported.

Similarity Metric	PMC (%)	Time (ms)
GeoS	86.64	0.148
MS	33.55	4.59
PS	46.61	5.62
DEPS	49.34	13.3
DEGS_16	25.31	458
DELS_25	30.44	44.1

To obtain the baseline performance of EBGM we extensively experiment with two of the promising EBGM variants in terms of speed and performance, following the general methodology described in (Pnevmatikakis and Polymenakos, 2005). The MS is the most promising of the fast variants, whereas DEGS_16 is the best and slowest variant. The MS and DEGS_16 variants are compared for different number of training images per class in Table 2. The PMC and ID time reported are averages across a large number of runs with different training and testing subsets. It is clear that DEGS_16 has consistently superior identification performance, although the discrepancy between the two methods is reduced as more training images per class become available. However, MS is considerably faster, being able to identify an image in about two orders of magnitude less time than DEGS_16. We can therefore propose two variants of the EBGM algorithm according to the metric used for identification. When identification time is critical (real-time applications), the best variant is MS, especially if many training images per class are available. However, when we are interested in the optimum recognition performance and have no serious time constraints (off-line applications) the most appropriate variant is definitely DEGS_16. This is considered the baseline performance for EBGM.

Table 2: Comparison of recognition and speed characteristics between the MS and DEGS_16 metrics.

TPC	Runs	PMC (%)		ID Time (sec)	
		MS	DEGS_16	MS	DEGS_16
2	300	19.79	14.87	0.011	0.957
3	400	13.84	10.24	0.016	1.578
5	400	8.55	6.15	0.032	3.168
10	400	4.84	3.06	0.048	5.164

The baseline performance of EBGM (DEGS_16) is compared to that of the linear subspace projection methods. PCA without the 3 eigenvectors that correspond to the largest eigenvalues (PCAw/o3) is used as a representative of the unsupervised projection estimation methods and PCA+LDA for the supervised projection estimation methods (Duda et al., 2000; Pnevmatikakis and Polymenakos, 2004). The same experiments have been run for the subspace projection methods and the averaged PMC is compared in Figure 4.

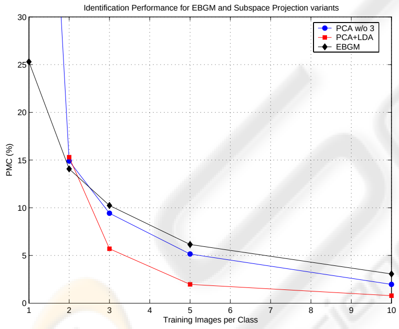

Figure 4: Comparison of the average PMC of EBGM (DEGS_16) and subspace projection methods (PCAw/o3 and PCA+LDA) as a function of the number of training images per class.

EBGM (DEGS_16) is superior when there is only a single training image per class, and somewhat better when there are two. For more than two its performance is worse than both subspace projection methods. Since PCA+LDA is even faster than the MS EBGM variant, obviously EBGM is not a good choice when adequate training is available, the conditions are approximately neutral (in terms of pose illumination and expression) and the normalization is based on the ideal eye positions.

5 EFFECT OF IMPAIRMENTS

Having established a baseline identification performance for EBGM under approximately neutral conditions and having identified it inferior to the PCA+LDA performance, we now attempt to identify the effect on that baseline of different preprocessing and impairments like small image size and imperfect eye positions. We also extend the comparison with PCA+LDA, to establish the relative performance of the two methods under less ideal conditions.

5.1 Effect of Preprocessing

It is argued in (Pnevmatikakis and Polymenakos, 2004; Bolme, 2003) that a different preprocessing scheme that involves making the images zero-mean and unit-variance is more appropriate when there are different illumination conditions in the images. Such differences exist in HumanScan, hence zero-mean and unit-variance preprocessing is applied. The faces in the resulting images are identified using the two EBGM variants and PCA+LDA.

The results for the two EBGM variants indicate that there is no clear advantage from the extra preprocessing step. More specifically, in a total of 25 runs using a single training image per class the average PMC improved only slightly (by 0.24% under MS and 0.03% under DEGS_16).

These tests were repeated for 300 runs with 2 training images per class under the DEGS_16 metric. The results are depicted as a scatter plot in Figure 5 and it is obvious that there is again no clear benefit in introducing intensity normalization to the preprocessing step: both the average and standard deviation of the PMC are practically unaffected. This is not the case for the PCA+LDA combination. The average PMC improves, and does so significantly when there are few training images per class. The individual runs are also shown as a scatter plot in Figure 5.

5.2 Effect of Image Size

The resilience of face recognition algorithms to small face sizes is very important in deployments where zoom cameras are not available. To investigate the effect of face size on identification performance, the HumanScan images are resized and the average PMC is again reported for the different sizes.

Figure 6 shows the effect of different image sizes on the recognition performance for a varying number of training images per class for MS EBGM and PCA+LDA. We can see that as the image size is reduced the PMC increases, which was to be expected since downscaling smears the facial characteristics and makes reliable fiducial point location harder. For

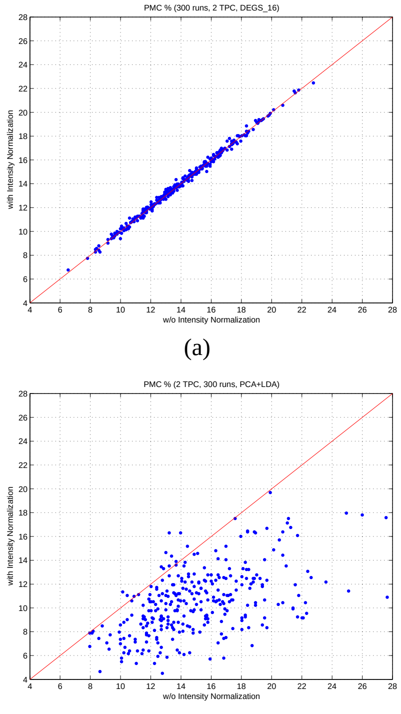

(a)

(b)

Figure 5: Using scatter plots to study the effect of pre-processing using intensity normalization for EBGM (a) and PCA+LDA (b).

EBGM, this degradation becomes less noticeable as more training images per class are used. This indicates that EBGM can withstand changes in scale quite well if the training set size is large enough.

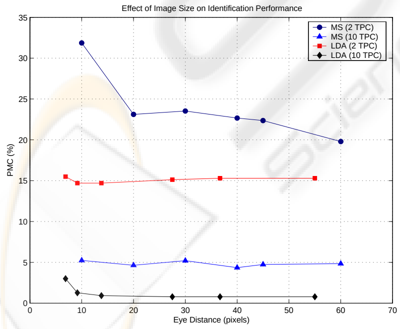

Figure 6: Effect of downsizing images for various training set sizes.

The opposite can be said for PCA+LDA. There the degradation is minor for 2 training images per class, but it becomes more noticeable in 10 training images per class. For extremely small face sizes, the performance of EBGM and PCA+LDA is comparable.

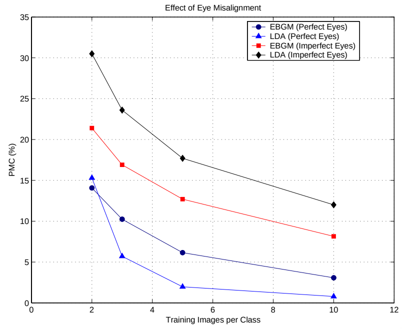

Figure 7: Effect of imperfect eye localization for various training set sizes.

5.3 Effect of Eye Misalignment

The subspace projection methods depend a lot on proper alignment of the images. Hence normalization is performed using the annotated eye positions. Unfortunately, in automatic face recognition systems the eye positions can only be estimated by some face detector. These estimates are not always very accurate. EBGM on the other hand does not in theory demand accurate eye positions; it takes advantage of the elasticity of the bunch graph to cope with eye misalignments. In this subsection, the eye positions estimated using an actual eye detector from unpublished work, which gives an RMS eye position error of 4.12% of the eye distance, are used to normalize the Human-Scan images. Then, the recognition performance of the EBGM (DEGS_16) and the subspace projection methods (LDA) is compared. The results are depicted in Figure 7. As expected, EBGM clearly outperforms PCA+LDA when the eyes are not ideally located.

6 CONCLUSIONS

In this paper we have first established a baseline performance for the EBGM algorithm for face recognition and compared it to the different subspace projection methods. We have shown that EBGM can be used to successfully locate the positions of fiducial points in novel images, even when only a few training images per class are contained in the FBG. We then studied two different metrics used in the recognition process, leading to two versions of EBGM that could be used in practice, depending on the particular application and its requirements in terms of speed and recognition accuracy. Finally, we compared EBGM to subspace projection methods with respect to different pre-processing schemes, different image sizes and imperfect eye localization. Even though PCA+LDA is faster and better performing than EBGM, we have established some application scenarios for EBGM. EBGM seems a very suitable choice when there is only one training image per class, and a reasonable choice when there are two. Even for more training images per class, EBGM should be used when the images are extremely small, or when the eyes are not ideally located.

A number of issues are still open. With regard to identification accuracy, it is clear that we need to utilize more appropriate metrics or enhance the existing ones. One way to approach this problem is to weigh the contribution of each fiducial feature by a different amount when computing the total similarity over the whole face. The major obstacle in this case is the determination of the appropriate weights in a systematic way. A simple idea is to weigh each contribution according to the expected accuracy in estimating the feature position, so that we bias our decision towards those fiducial points we have more confidence in.

Another way of improving performance would be to use a larger number of fiducial points for each image, by interpolating between the positions of the known features. For example, 25 original points and 55 interpolated points have been used in (Bolme, 2003) to construct each Face Graph, while we have used only the 20 points originally defined by HumanScan. The main concern here is to avoid using too many and closely spaced points, as that would degrade identification accuracy (Wiskott et al., 1999). Our early experiments show that adding just one extra point can improve average performance by about 1%, but some of the tried extra points can degrade performance by three times as much.

The choice of kernel sizes is also very important as images are downsized, since the use of smaller kernels would reduce correlation between convolution results from neighboring jets. Ideally, we would like to have an algorithm that can dynamically adapt to the image dimensions and adjust the size and composition of the kernel set accordingly.

ACKNOWLEDGEMENTS

This work is partly sponsored by the EU under the Integrated Project CHIL, contract number 506909.

REFERENCES

Belhumeur, P., Hespanha, J., and Kriegman, D. (1997). Eigenfaces vs. fisherfaces: Recognition using class specific linear projection. *IEEE Trans. Pattern Analysis and Machine Intelligence*, 19(7):711–720.

Beveridge, J. and She, K. (2001). Fall 2001 update to CSU PCA versus PCA+LDA comparison. Technical report, Colorado State University, Fort Collins, CO.

Bolme, D. S. (2003). Elastic Bunch Graph Matching. Master's thesis, Computer Science Department, Colorado State University.

Brunelli, R. and Poggio, T. (1993). Face recognition: Features versus templates. *IEEE Trans. Pattern Analysis and Machine Intelligence*, 15:1042–1052.

Christmas, B. and Galambos, C. (2005). `http://www.ee.surrey.ac.uk/Research/VSSP/RavlDoc/share/doc/RAVL/Auto/Basic/Tree/Ravl.html`.

Duda, R., Hart, P., and Stork, D. (2000). *Pattern Classification*. Wiley-Interscience, New York.

Georghiades, A., Belhumeur, P., and Kriegman, D. (2001). From few to many: Illumination cone models for face recognition under variable lighting and pose. *IEEE Trans. Pattern Analysis and Machine Intelligence*, 23(6):643–660.

Gunning, J. and Murphy, N. (1992). Neural network based classification using automatically selected feature sets. *IEE Conf. Series 359*, pages 29–33.

Jesorsky, O., Kirchberg, K., and Frischholz, R. (2001). Robust face detection using the Hausdorff distance. In *Audio and Video based Person Authentication - AVBPA 2001*, pages 90–95. Springer.

Martinez, A. and Kak, A. (2001). PCA versus LDA. *IEEE Trans. Pattern Analysis and Machine Intelligence*, 23(2):228–233.

Pentland, A., Moghaddam, B., and Starner, T. (1994). View-based and modular eigenspaces for face recognition. *Proc. IEEE Conf. on Comp. Vision & Pattern Rec.*, pages 84–91.

Pnevmatikakis, A. and Polymenakos, L. (2004). Comparison of eigenface-based feature vectors under different impairments. *Int. Conf. Pattern Recognition 2004*, 1:296–300.

Pnevmatikakis, A. and Polymenakos, L. (2005). A testing methodology for face recognition algorithms. In *2nd Joint Workshop on Multi-Modal Interaction and Related Machine Learning Algorithms, Edinburgh*.

Turk, M. and Pentland, A. (1991). Eigenfaces for recognition. *J. Cognitive Neuroscience*, 3:71–86.

Waibel, A., Steusloff, H., and Stiefelhagen, R. (2004). CHIL - Computers in the Human Interaction Loop. In *5th International Workshop on Image Analysis for Multimedia Interactive Services - WIAMIS 2004*.

Wiskott, L., Fellous, J.-M., Krueger, N., and von der Malsburg, C. (1999). Face recognition by Elastic Bunch Graph Matching. In *Intelligent Biometric Techniques in Fingerprint and Face Recognition*, chapter 11, pages 355–396. CRC Press.

Yang, M., Kriegman, D., and Ahuja, N. (2002). Detecting faces in images: A survey. *IEEE Trans. Pattern Analysis and Machine Intelligence*, 24(1):34–58.

Zhao, W., Chellappa, R., Rosenfeld, A., and Phillips, P. (2000). Face recognition: A literature survey.